

Short Communication

Designing a high-throughput viscous heater to process feces: heater geometry

Jagdeep T. Podichetty, Gary L. Foutch, A. H. Johannes, Jim Smay and Md. Waliul Islam

ABSTRACT

Viscous heating technology can destroy disease-causing microorganisms with no additional heat input. A laboratory-scale unit was constructed and tested with a simulant, and viscous heating achieved temperatures as high as 190 °C. This study discusses additional variables – length and spacing – that are important to process design and optimization. The viscosity (μ) was described as a function of shear rate ($\dot{\gamma}$); $\mu = 140$ Pa s for $t = 0$ s and $\mu = 32 * (\dot{\gamma})^{-0.6}$ Pa s for $t > 0$ s. The advantages of viscous heating to sanitize fecal mass are presented. The results show temperature gradient is more sensitive to changes in gap spacing than reactor length. For high throughput, the viscous heater length must be increased to provide fluid sufficient residence time to achieve the desired effluent temperature.

Key words | computational fluid dynamics, extrusion, feces, parasite, viscosity, viscous heating

Jagdeep T. Podichetty

A. H. Johannes

Md. Waliul Islam

Chemical Engineering, Oklahoma State University,
Stillwater, OK 74078,
USA

Gary L. Foutch (corresponding author)

Computing and Engineering,
University of Missouri Kansas City, MO 64110,
USA

E-mail: foutch@okstate.edu

Jim Smay

Materials Science and Engineering,
Oklahoma State University Tulsa, OK 74106,
USA

INTRODUCTION

Worldwide, 2.5 billion people lack basic sanitation ([World Health Organization 2014](#)). Inadequate sanitation is responsible for spreading diarrheal diseases through contaminated water. In addition, 11% of the world's population, about 780 million people, in less developed regions remain without access to safe drinking water ([United Nations 2012](#)). People are exposed to pathogens by contact with contaminated water and soil by several mechanisms: through storm water runoff, septic tank leakage, sanitary sewer system breakage and overflow, and improper disposal of human and animal feces ([Santo Domingo et al. 2007](#)).

Parasites in feces include helminthes and protozoa. Particular interest focuses on *Ascaris lumbricoides*, *Trichuris trichiura*, *Taenia* spp., *Giardia intestinalis*, and *Cryptosporidium* spp. ([Tronnberg et al. 2010](#)). The helminth (parasitic worms) infections in the human digestive track are ascariasis (giant roundworm), trichuriasis (whipworm), and hookworm. Helminthes eggs in feces of infected people

contaminate soil and are transmitted by contact. Protozoan diseases are numerous and include amoebiasis and giardiasis. Protozoan cysts and oocysts have several known feces-to-mouth transmission mechanisms ([Centers for Disease Control & Prevention \(CDC\) 2013](#)). These diseases cause not only physical harm and death, but also reduce cognitive development ([Bethony et al. 2006](#)).

[Podichetty et al. \(2014\)](#) describe the use of computational fluid dynamics (CFD) for preliminary design of a viscous heating device to raise the temperature of solid wastes sufficient to inactivate disease-causing microbes. Comsol Multiphysics v4.3 (C-M) was used to solve and analyze energy and mass balances within alternative geometries. After CFD analysis was completed a viscous heater was built and tested. A parametric study of the performance of the viscous heater is described by [Podichetty et al. \(2014\)](#). This paper continues that discussion for additional reactor variables and their design and optimization impact.

MATERIALS AND METHODS

Reactor geometry

A geometric representation of the viscous heater was built using computer-aided design. R_i and R_o are the inner and outer radius of the cylinders, respectively. A no-slip boundary condition was applied at the outer cylinder with initial conditions of 0 Pa gage pressure and 298 K. The outer surface of the viscous heater was set to a fixed temperature or insulation. The viscous heater was assumed to be high-strength alloy steel with associated thermal properties. The spacing of the viscous heater can be adjusted by changing the inner cylinder radius.

The viscous heater geometry is symmetric around the actual axis of the inner, rotating cylinder. Hence, a 2D cross-section was created and then extended to represent the 3D geometry (Figure 1). The viscous heater cross-sectional geometry was meshed with a total of 380,000 domain nodes with a mesh area of 0.028 m². Increasing the number of nodes had no significant effect on temperature predictions: less than 0.1% change in temperature values. Hence, simulations were performed with 380,000 domain nodes for computational simplicity.

Governing equations

Modeling the viscous heater process involves three elements: an ability to solve 3D flow equations; an accurate viscosity model; and an objective function (Podichetty *et al.* 2014). The phenomenon of viscous heating is a result of molecular friction that converts mechanical energy into heat.

An accurate description of the temperature distribution within the flowing mass involves simultaneous solution of the fluid flow and heat transfer models.

An accurate viscosity model representing the non-Newtonian fluid behavior of fecal sludge is critical in predicting the local rate of heat generation by viscous heating since this rate depends both on the local shear rate ($\dot{\gamma}$) and the viscosity (μ) of the fluid (Woolley *et al.* 2013). Hence, the viscosity model should extend over the full $\dot{\gamma}$ range observed throughout the process. Some of the viscosity models used widely include power-law, Carreau-Yasuda, and Bird-Carreau, and Cross (Gifford 1997; Vlachopoulos & Strutt 2003). Governing equations for conservation of mass, heat transfer, viscous heating, and pressure work were based on Podichetty *et al.* (2014).

The fluid and material properties used are listed in Table 1. The feed is assumed to enter the viscous heater at room temperature. The simulations were performed at 1,800 rpm. The viscosity (μ) was described as a function of shear rate ($\dot{\gamma}$) as shown in Table 1. The viscosity model ignores the effect of temperature because insufficient experimental data were available for feces, but in practice viscosity decreases with an increase in temperature. A model that includes the viscosity–temperature relationship would show lower predicted effluent temperatures. However, as noted in Podichetty *et al.* (2014), experimental data and the CFD simulation match reasonably well without a more sophisticated viscosity model. The time dependent simulations were performed for 200 s using a stationary, ‘Fully Coupled’ solver configuration (COMSOL Multiphysics 2012). The fully coupled solver uses the initial guesses and applies Newton–Raphson iterations until the solution

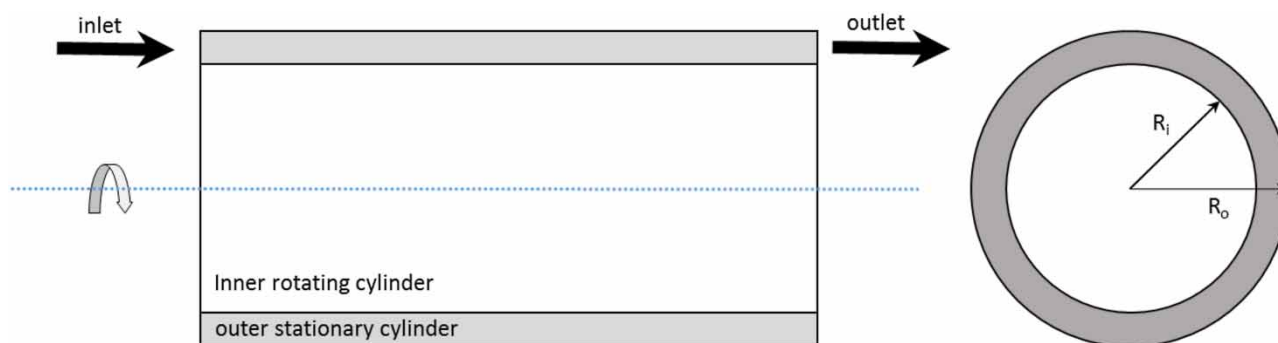


Figure 1 | Cylindrical viscous heater geometry.

Table 1 | Fluid and material properties used for modeling

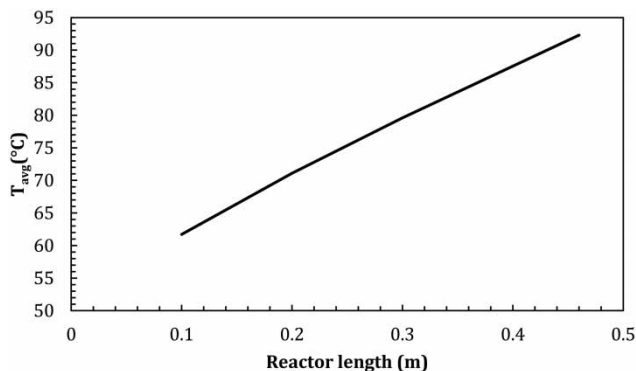
Red potato	
Density, ρ	1,030 kg/m ³
Viscosity model, μ	140 Pa s; $t = 0$ s $32 \times (\text{Shear rate})^{-0.6}$ Pa s; $t > 0$ s
Thermal conductivity, k	0.03 W/(m K)
Heat capacity, C_p	4,186 J/(kg K)
High-strength alloy steel	
Heat capacity, C_p	475 J/(kg K)
Thermal conductivity, k	44.5 W/(m K)
Density, ρ	7,850 kg/m ³

converges. The solver computes the large sparse system of equations in parallel to reduce computation time.

RESULTS AND DISCUSSION

Viscous heater length

Parameters such as viscous heater length (L) and \dot{m} can be used to regulate T_{avg} . CFD analysis was performed to understand the effect of L on T_{avg} in the range from 0.1 to 0.46 m. The $T_{\text{s,ext}}$ was fixed to 370 °C. As expected, T_{avg} increases with increasing viscous heater length (Figure 2). Increase in length increases the fluid residence time, allowing the fluid to achieve higher temperature. Increasing the feed flow rate allows more feces to be processed quickly. However, the reactor length must be extended accordingly to provide sufficient residence time for the fluid to achieve the desired temperature.

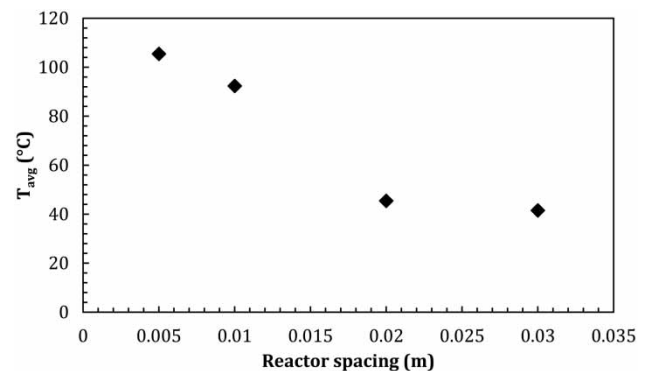
**Figure 2** | T_{avg} at different viscous heater length.

Spacing

The spacing between the cylinders can be adjusted by varying the diameter of the inner cylinder. The CFD results showed a decrease in average temperature with an increase in spacing. Increasing the spacing results in an increase in holdup volume, which reduces the average temperature. For higher spacing, increasing the residence time may help achieve higher temperatures. However, increasing the spacing above 0.02 m did not show significant variation in T_{avg} as the viscous heater did not achieve higher temperature (Figure 3). Care must be taken to avoid larger solid particles entering the spacing that could block the flow or damage the cylinder surface. Prescreening of feed is recommended to ensure consistency in particle size entering the viscous heater.

CONCLUSION

CFD was used to analyze a viscous heating device and study the effects of design parameters, reactor length and spacing, on the temperature profile of a high-viscosity fluid. For a 0.46 m long viscous heater, the results showed that the temperature gradient depends significantly on spacing. At higher flow rate, the viscous heater length should be extended to provide the fluid sufficient residence time to achieve the desired effluent temperature. This CFD model has proved useful in designing a viscous heater for a specific feed rate and operating temperature. In addition, the CFD model can be extended to include other factors such as heat loss to the surroundings or auxiliary heat input. The design can

**Figure 3** | Average temperature in the viscous heater at different spacing (simulated).

be used as a stand-alone operation or be linked with other fecal mass processing technologies.

ACKNOWLEDGEMENTS

Funding for this work was provided by the Bill & Melinda Gates Foundation. The authors would like to thank Yang Shi, Jennifer Thomas, Robert Dunlap, Drew Belcher, and Kathleen McNamara for providing the viscosity data.

REFERENCES

- Bethony, J. S., Brooker, M., Albonico, S. M., Geiger, A., Loukas, D., Diemert, R. J. & Hotez, P. J. 2006 Soil-transmitted helminth infections: ascariasis, trichuriasis, and hookworm. *Lancet* **367** (9521), 1521–1532.
- Centers for Disease Control, Prevention (CDC) 2013 *Cryptosporidium*. www.cdc.gov/parasites/crypto/ (accessed 5 April 2015).
- COMSOL MULTIPHYSICS 2012 *COMSOL Multiphysics User's Guide, Version 4.3*. Stockholm, Sweden, pp. 1225–1226.
- Gifford, W. A. 1997 The use of three dimensional computational fluid dynamics in design of extrusion dies. *J. Reinf. Plast. Compos.* **16**, 661–674.
- Podichetty, J. T., Islam, Md., Van, D., Foutch, G. L. & Johannes, A. H. 2014 Viscous heating analysis of simulant feces by CFD and experimentation. *J. Water, San. Hyg. Dev.* **4** (1), 62–71.
- Santo Domingo, J. W., Lu, J., Shanks, O. C., Lamendella, R., Kelty, C. A. & Oerther, D. B. 2007 Development of host-specific metagenomic markers for microbial source tracking using a novel metagenomic approach. *Disinfection* **16**, 646–661.
- Trönnberg, L., Hawksworth, D., Hanses, A., Archer, C. & Stenstrom, T. A. 2010 Household-based prevalence of helminths and parasitic protozoa in rural KwaZulu-Natal, South Africa, assessed from faecal vault sampling. *Trans. Royal Soc. Trop. Med. Hyg.* **104** (10), 646–652.
- United Nations 2012 *The Millennium Development Goals Report*. <http://www.un.org/millenniumgoals/pdf/MDG%20Report%202012.pdf> (accessed 29 August 2014).
- Vlachopoulos, J. & Strutt, D. 2003 The role of rheology in polymer extrusion. In: *New Technologies for Extrusion Conference*, Milan, Italy.
- Woolley, S., Buckley, C., Pocock, J., Cottingham, R. & Foutch, G. 2013 Some rheological properties of fresh human feces with a variation in moisture content & rheological modeling of fresh human feces. In: *3rd SA YWP Conference*, Stellenbosch, Western Cape, South Africa.
- World Health Organization 2014 *Investing in Water and Sanitation: Increasing Access, Reducing Inequalities, (GLAAS) 2014 – Report*. www.who.int/water_sanitation_health/publications/glaas_report_2014/en/ (accessed 5 April 2015).

First received 10 November 2014; accepted in revised form 6 April 2015. Available online 21 May 2015